Anaerobic methane oxidation in an East African great lake (Lake Kivu)

Fleur A. E. Roland[1]*, François Darchambeau[1], Cédric Morana[2], Sean A. Crowe[3], Bo Thamdrup[4], Jean-Pierre Descy[1,5] and Alberto V. Borges[1]

[1] Chemical Oceanography Unit, Université de Liège, Belgium

[2] Department of Earth and Environmental Sciences, Katholieke Universiteit Leuven (KU Leuven), Belgium

[3] Department of Earth, Ocean and Atmospheric Sciences, University of British Columbia, Canada

[4] Institute of Biology and Nordic Center for Earth Evolution, University of Southern Denmark, Denmark

[5] Laboratory of freshwater ecology, URBO, Department of Biology, Université de Namur, Belgium

* *Corresponding author*: froland@ulg.ac.be

Abstract

This study investigates methane (CH_4) oxidation in the water column of Lake Kivu, a deep meromictic tropical lake containing large quantities of CH_4 in the anoxic deep waters. Depth profiles of dissolved gases (CH_4 and nitrous oxide (N_2O)) and of the different potential electron acceptors for anaerobic methane oxidation (AOM) (nitrate, sulfate, iron and manganese) were determined during six field campaigns between June 2011 and August 2014. Denitrification measurements based on stable isotopes were performed twice. Incubation experiments were performed to quantify CH_4 oxidation and nitrate consumption rates, with a focus on AOM, without and with an inhibitor of sulfate-reducing bacteria activity (molybdate). Nitrate consumption rates were measured in these incubations during all field campaigns, and sulfate consumption rates were measured in August 2014. CH_4 production was also measured in parallel incubations by addition of picolinic acid, an inhibitor of CH_4 oxidation, during three field campaigns, with rates up to 370 nmol L^{-1} d^{-1}. Substantial CH_4 oxidation activity was observed in oxic and anoxic waters, and in the upper anoxic waters of Lake Kivu, CH_4 is a major electron donor to sustain anaerobic metabolic processes coupled to AOM. The maximum aerobic and anaerobic CH_4 oxidation rates were estimated to 27 ± 2 and 16 ± 8 µmol L^{-1} d^{-1}, respectively. We observed a decrease of AOM rates when molybdate was added for half of the measurements, strongly suggesting the occurrence of AOM linked to sulfate reduction, but an increase of AOM rates was observed for the other half. Nitrate reduction rates and dissolved manganese production rates tended to be higher with the addition of molybdate, but the maximum rates of 0.6 ± 0.02 and 11 ± 2 µmol L^{-1} d^{-1}, respectively, were not high enough to explain AOM rates observed at the same depths. We also put in evidence a difference in the relative importance of aerobic and anaerobic CH_4 oxidation between the seasons, with a higher importance of aerobic oxidation when the oxygenated layer was thicker (in the dry season).

1. Introduction

Due to its potential impact in global warming and its increase due to human activities, the biogeochemical cycle of methane (CH_4) raises great interest, and methanogenesis and methanotrophy have been widely studied in a large variety of environments. In natural environments, CH_4 is produced anaerobically by methanogenic archaea. Recent studies also suggest that CH_4 can be produced in oxic conditions, by oxygen tolerant methanogenic archaea coupled to phytoplankton activity (Grossart et al., 2011;Bogard et al., 2014;Tang et al., 2014;Tang et al., 2016). The total CH_4 emission has been recently estimated to 553 Tg CH_4 yr^{-1} for the period 2000-2009, from which 64 % is emitted by tropical areas (Kirschke et al., 2013;Saunois et al., 2016). Decadal variations in the annual atmospheric CH_4 growth rate have also been attributed to changes in emissions from tropical wetlands (Nisbet et al., 2016). Previous studies estimated that 9.5% of CH_4 is released from tropical freshwaters and the rest from non-tropical freshwaters (13.5%), marine ecosystems (3%), human activities (63%), plants (6%), gaseous hydrates (2%) and termites (3%) (Conrad, 2009;Bastviken et al., 2011). The real amount of CH_4 produced in these systems is higher, but a significant percentage is biologically oxidized (aerobically or anaerobically) before reaching the atmosphere (Bastviken et al., 2002). Anaerobic CH_4 oxidation (AOM) has been widely observed in marine environments, where it is mainly coupled to sulfate (SO_4^{2-}) reduction (e.g. Iversen and Jørgensen, 1985;Boetius et al., 2000;Jørgensen et al., 2001). Comparatively, in situ AOM has been less frequently measured in freshwaters environments (e.g. in Lake Rotsee; Schubert et al., 2010), and is often considered as negligible compared to aerobic CH_4 oxidation due to lower SO_4^{2-} concentrations than in seawater (Rudd et al., 1974). However, other potential electron acceptors for AOM, such as nitrate (NO_3^-), iron (Fe) and manganese (Mn) (Borrel et al., 2011;Cui et al., 2015), can be found in non-negligible concentrations in freshwater environments. AOM coupled to NO_3^- reduction (NDMO) has been exclusively observed in laboratory environments (e.g. Raghoebarsing et al., 2006;Ettwig et al., 2010;Hu et al., 2011;Haroon et al., 2013;á Norði and Thamdrup, 2014), and its natural significance is still unknown. Also, AOM coupled to Fe and Mn reduction has been proposed to occur in some freshwater environments (e.g. in lakes Matano and Kinneret; Crowe et al., 2011;Sivan et al., 2011;á Norði et al., 2013) and marine sediments (Beal et al., 2009), but to our best knowledge, no in situ measurements have been reported in the literature.

Lake Kivu is a deep (maximum depth: 485 m) meromictic lake characterized by a high amount of CH_4 (60 km^3 at 0°C and 1 atm) dissolved in its deep anoxic waters. Paradoxically, this lake is a very low emitter of CH_4 to the atmosphere due to intense CH_4 oxidation (Borges et al., 2011;Roland et al., 2016a). It is divided in different basins and bays. In the water column of the main basin, SO_4^{2-} concentrations are relatively high (100-200 µmol L^{-1}; Morana et al., 2016) and a large SO_4^{2-}-reducing bacteria (SRB) community is present and co-occurs with methanotrophic archaea (İnceoğlu et al., 2015). The data based on 16S rRNA strongly suggest the occurrence of AOM coupled to SO_4^{2-} reduction (SDMO), although it remains to be demonstrated in a direct way and quantified. Also, a NO_3^- accumulation zone (nitracline) is often present during the rainy season at the oxic-anoxic interface (Roland et al., 2016a), and can potentially contribute to AOM. Based on these observations, we hypothesize that SO_4^{2-} could be the unique electron acceptor involved in AOM during the dry season, while AOM coupled with NO_3^- reduction (NDMO) could also contribute during the rainy season at a lower extent. Potential AOM linked to Fe and Mn reduction will also be investigated. In order to fully investigate CH_4 cycle in the water column of Lake Kivu, we also measured CH_4 production in the oxic compartment.

2. Material and methods

2.1 Sampling sites

Lake Kivu is an East African great lake located at the border between Rwanda and the Democratic Republic of the Congo (Fig. 1). It is divided into one main basin, two small basins and two bays: Northern Basin (or main basin), Southern Basin (or Ishungu Basin), Western Basin (or Kalehe Basin), the bay of Kabuno in the north and the bay of Bukavu in the South.

Six field campaigns were conducted in the main basin (the Northern Basin off Gisenyi; -1.72504°N, 29.23745°E) in June 2011 (early dry season), February 2012 (rainy season), October 2012 (late dry season), May 2013 (late rainy season), September 2013 (dry season) and August 2014 (dry season).

2.2 Physico-chemical parameters and sampling

Vertical profiles of temperature, conductivity, pH and oxygen were obtained with a Yellow Springs Instrument 6600 V2 multiparameter probe. Water was collected with a 7L Niskin bottle (Hydro-Bios) every 2.5 m in a ~10 m zone centered at the oxic-anoxic interface.

2.3 Chemical analyses

Samples for CH_4 and N_2O concentrations, and CH_4 oxidation measurements were collected in 60 ml glass serum bottles, filled directly from the Niskin bottle with tubing, left to overflow, and sealed with butyl stoppers and aluminium caps. Two bottles were directly poisoned with 200 µl of $HgCl_2$ injected through the septum with a syringe. Ten other bottles were incubated in the dark and at constant temperature close to in situ temperature (~23°C). Five of them received 250 µl of a solution of sodium molybdate, an inhibitor of sulfate-reducing bacteria activity (1 mol L^{-1}; hence a final concentration of 4 mmol L^{-1}), and five received no treatment. In May 2013, September 2013 and August 2014, five supplementary bottles received 500 µl of a solution of picolinic acid, an inhibitor of CH_4 oxidation (6 mmol L^{-1}; final concentration of 0.1 mmol L^{-1}). The bacterial activity of these ten bottles was stopped at 12, 24, 48, 72 and 96h by the addition of 200 µl of a saturated solution of $HgCl_2$. CH_4 and N_2O concentrations were determined via the headspace equilibration technique (20 mL N_2 headspace in 50 mL serum bottles, for samples of the main basin) and measured by gas chromatography (GC) (Weiss, 1981) with electron capture detection (ECD) for N_2O and with flame ionization detection (FID) for CH_4, as described by (Borges et al., 2015). The SRI 8610C GC-ECD-FID was calibrated with certified CH_4:CO_2:N_2O:N_2 mixtures (Air Liquide, Belgium) of 1, 10, 30 and 509 ppm CH_4 and of 0.2, 2.0 and 6.0 ppm N_2O. Concentrations were computed using the solubility coefficients of Yamamoto et al. (1976) and Weiss and Price (1980), for CH_4 and N_2O, respectively. The precision of measurements was ±3.9% and ±3.2% for CH_4 and N_2O, respectively.

Samples for nutrients analyses were collected in 50 ml plastic vials after being filtered through a 0.22 µm syringe filter. 200 µl of H_2SO_4 5N were added at each vial for preservation. Samples were then frozen. NO_2^- and NO_3^- concentrations were estimated by spectrophotometry. NO_2^- concentrations were determined by the sulfanilamide coloration method (APHA 1998), using a 5-cm light path on a spectrophotometer Thermo Spectronic Genesys 10vis. NO_3^- concentrations were determined after vanadium reduction to NO_2^- and quantified under this

form with a Multiskan Ascent Thermo Scientific multi-plates reader (APHA, 1998;Miranda et al., 2001). The detection limits for these methods were 0.03 and 0.15 µmol L^{-1} for NO_2^- and NO_3^-, respectively. When making the headspaces for CH_4 measurements as described above, the excess water was collected and used to quantify the evolution of NO_3^- concentrations in the incubations (reported as NO_3^- consumption rates), according to the method previously described.

Samples for sulfide (HS^-) concentrations were collected in 50 ml plastic vials, after being filtered on a 0.22 µm syringe filter. Samples were preserved with 200 µl of 20% zinc acetate (ZnAc) and were stored frozen. HS^- concentrations were quantified using a 5-cm light path on a spectrophotometer, according to the method described by Cline (1969). Samples for SO_4^{2-} analyses were filtered through a 0.22 µm syringe filter and collected in 5 ml Cryotube vials. Samples were preserved with 20 µl of 20% ZnAc and were stored frozen. SO_4^{2-} concentrations were determined by ion chromatography (Dionex ICS-1500, with an autosampler Dionex AS50, a guard column Dionex AG22 and an analytical column Dionex IonPac AS22). The detection limits of these methods were 0.25 and 0.5 µmol L^{-1} for HS^- and SO_4^{2-}, respectively. In August 2014, the decrease of SO_4^{2-} concentrations in CH_4 incubations was measured by spectrophotometry, using a 5-cm light path on a spectrophotometer Thermo Spectronic Genesys 10vis, according to the nephelometric method described by Rodier et al. (1996), after precipitation of barium sulfate in an acid environment. The detection limit of this method was 52 µmol L^{-1}.

In May 2013, September 2013 and August 2014, samples for Fe and Mn measurements were collected into 50 ml-plastic syringes directly from the Niskin bottle. Water was rapidly transferred from the syringe to the filtration set and was passed through 25 mm glass fiber filters. Filters were collected in 2 ml Eppendorf vials and preserved with 1 ml of a HNO_3 2% solution, while filtrates were collected into four 2 ml Eppendorf vials and preserved with 20 µl of a HNO_3 65% solution. The filters, for particulate Fe and Mn determination, were mineralized in specific Teflon bombs into a microwave digestion labstation (Ethos D, Milestone Inc.), after digestion with nitric acid. They were finally diluted into milli-Q water to the volume of 50 ml. Filtrates were directly diluted into milli-Q water to the volume of 50 ml. In August 2014, dissolved Mn and Fe concentrations were also determined in CH_4 incubations in order to measure the evolution of concentrations through time. Fe and Mn concentrations were determined by inductively coupled plasma mass spectrometry (ICP-MS) using dynamic reaction cell (DRC) technology (ICP-MS SCIEX ELAN DRC II, PerkinElmer inc.). Analytical accuracy was verified by a certified reference material (BCR 715, Industrial Effluent Wastewater).

2.4 CH_4 oxidation and production, NO_3^- and SO_4^{2-} consumption and Mn^{2+} production rates calculations

CH_4 oxidation and production, NO_3^- and SO_4^{2-} consumption and Mn^{2+} production rates were calculated as a linear regression of CH_4, NO_3^-, SO_4^{2-} and Mn^{2+} concentrations over time during the course of the incubation. Rates reported here are maximum rates, as they were calculated based on the maximum slopes. Table 1 shows standard deviations, initial CH_4 concentrations, percentage of CH_4 consumed and the time laps during which the CH_4 oxidation rates were calculated for each depth. Table 2 shows standard deviations for NO_3^- and SO_4^{2-} consumption and Mn^{2+} production rates.

CH_4 oxidation rates with molybdate were corrected taking into account the oxygen supplied by the addition of the solution, which was not anoxic. As molybdate solution was at saturation with respect to O_2, we considered here that 1.25 µmol L^{-1} of O_2 were added to each bottle (250 µl of the solution were added to 60 ml of

water). The O_2 concentration required to be responsible for each CH_4 oxidation rate was calculated according to the following stoichiometric equation Eq. (1):

(1) $CH_4 + 2\ O_2 \rightarrow CO_2 + 2\ H_2O$

The part of each oxidation rate due to O_2 was then calculated according to Eq. (2):

(2) $Ro = Rm * (O_{2r}/O_{2a})$

where Ro is the part of each oxidation rate due to O_2 supply, Rm is the measured oxidation rate, O_{2r} is the O_2 concentration required to be responsible for the measured CH_4 oxidation rate and O_{2a} is the O_2 concentration added by the molybdate solution.

The final CH_4 oxidation rates with molybdate were obtained by subtraction (Eq. 3):

(3) Final CH_4 oxidation rate with Mo = Rm – Ro

All rates with molybdate reported here are final CH_4 oxidation rates.

2.5 N stable isotope labelling experiments

In May and September 2013, parallel denitrification experiments were conducted in order to link this process with CH_4 oxidation. Water was collected in duplicate in amber 250 ml borosilicate bottles from the Niskin bottle with tubing, left to overflow, and sealed with Teflon-coated screw caps. Before the injection of ^{15}N-labeled solutions, a 12h pre-incubation period in the dark and at 25°C was observed in order to allow the consumption of oxygen eventually introduced in the bottles during sampling.

N stable isotope labelling experiments were based on Thamdrup and Dalsgaard (2002). Heterotrophic denitrification was determined by the injection of a $Na^{15}NO_3$ solution in amber bottles, through the stopper (final concentration of 5 µmol L^{-1}). Six 12 ml vials (Labco Exetainer) were then filled from each of the duplicate bottles and placed in the dark in an incubator at ambient temperature (24°C), which was close to the in situ temperature (~23°C). Microbial activity in two Exetainers was immediately arrested through the addition of 500 µl 20% ZnAc. A time course was established by arresting two further Exetainers at 6, 12, 18, 24 and 48 h. While injecting ZnAc solution to stop the incubations of the Exetainers, the excess water was collected in 2 ml-Eppendorf vials, and stored frozen, to determine the evolution of the NO_x^- concentrations through time. NO_x^- were then analyzed by chemiluminescence, after reduction with vanadium chloride (VCl_3), with an NO_2^-, NO_3^- and NO_x analyzer (Thermo Environmental Instruments), according to the method described by Braman and Hendrix (1989) (detection limit: 2-3 ng NO_x).

$^{29}N_2$ and $^{30}N_2$ concentrations in the Exetainers were measured with a gas source isotope ratio mass spectrometer (Delta V Plus, ThermoScientific) after creating a 2 ml helium headspace (volume injected in the mass spectrometer: 50 µl). Potential denitrification rates (detection limits of 2.7 nmol L^{-1} h^{-1}) in the incubations with $^{15}NO_3^-$ were calculated according to Eq. (4) (Thamdrup and Dalsgaard, 2002):

(4) Potential $N_{2\ denitrification} = {}^{15}N^{15}N_{excess} * (F_{NO3})^{-2}$

where $N_{2\ denitrification}$ is the production of N_2 by denitrification during the incubations with $^{15}NO_3^-$. $^{15}N^{15}N_{excess}$ is the production of excess $^{15}N^{15}N$ and F_{NO3} is the fraction of $^{15}NO_3^-$ added in the NO_x^- pool. NO_x^- concentrations of the NO_x^- pool were measured in the incubations as described above. $^{15}N^{15}N$ is the excess relative to the mass 30: mass 28 ratio in the time zero gas samples.

Only natural denitrification rates are reported here. Natural denitrification rates were calculated on the base on potential denitrification rates, according to Eq. (5):

$$(5)\quad \text{Natural } N_{2\ denitrification} = \text{Potential } N_{2\ denitrification} * (1 - F_{NO3}),$$

which assumes that the rate obeys 1st order kinetics with respect to NO_3^-.

2.6 Pigment analysis

In May 2013, September 2013 and August 2014, samples for pigments analyses were collected on Whatman GF/F 47 mm glass fiber filters (filtration volumes: 3L). Filters were preserved in 5 ml Cryotube vials and stored frozen until pigment extraction in 4 ml of 90% HPLC grade acetone. Two 15-min sonications separated by an overnight period at 4°C in dark were applied, and extracts were stored in 2 ml-amber borosilicate vials. HPLC analyses were carried out as described by Sarmento et al. (2006).

3. Results

3.1 Physico-chemical characteristics of the water column

Vertical profiles of physico-chemical variables differed strongly between stations and campaigns (Fig. 2). In the dry season, the water column was anoxic from 47.5, 57.5, 55 and 60 m in June 2011, October 2012, September 2013 and August 2014, respectively. During the rainy season, it was anoxic from 45 and 55 m in February 2012 and May 2013, respectively. At each date, the thermocline and chemocline (based on specific conductivity and pH) mirrored the oxycline and temperature at the oxic-anoxic interface averaged 23.5 ± 0.2°C (mean ± standard deviation).

CH_4 concentrations were low (0.3 ± 0.5 µmol L^{-1}) from the surface to 45-55 m where they started to increase; at 70 m, CH_4 concentrations were 385 ± 43 µmol L^{-1} (Fig. 3). For all campaigns, N_2O concentrations were higher in oxic waters (7.0 ± 0.4 nmol L^{-1} from 0-40 m) than in anoxic waters (1.3 ± 0.8 nmol L^{-1} below 60 m depth). In February 2012 and September 2013, peaks of N_2O up to 15 nmol L^{-1} were observed at 50 m (anoxic waters) and at 45 m (oxic waters), respectively.

NO_x profiles also reflected the seasonal variations of the water column characteristics. A zone of NO_x accumulation (nitracline) was not observed in June 2011 and May 2013, and a small one (<2 µmol L^{-1} at 52.5 m) was observed in August 2014. In February 2012, October 2012 and September 2013, NO_x maxima of 3 µmol L^{-1} (at 50 m), 4 µmol L^{-1} (at 50 m) and 4 µmol L^{-1} (at 47.5 m), respectively, were observed. SO_4^{2-} and H_2S concentrations did not show high fluctuations between the different campaigns. The mean of SO_4^{2-} concentrations in oxic waters (from 0 to 50 m depth) was 153 ± 21 µmol L^{-1}, while the mean of H_2S concentrations in anoxic waters (at 70 m depth) was 42 ± 25 µmol L^{-1}. SO_4^{2-} concentrations strongly decreased in the anoxic zone (until ~0 µmol L^{-1} at 80 m depth), while HS^- concentrations increased.

While particulate Fe concentrations were up to 15 µmol L^{-1} in oxic waters, in September 2013, dissolved Fe concentrations were very low (less than 2.5 µmol L^{-1} all along the vertical profiles, during the three field campaigns). On the contrary, particulate Mn concentrations were low (less than 2 µmol L^{-1}), with a maximum concentration peak located just above the oxic-anoxic interface, for the three campaigns, and dissolved Mn concentrations increased with depth, until maximum concentrations of 10 µmol L^{-1} in anoxic waters.

3.2 Microbial process rate measurements

CH_4 oxidation was detected during all field campaigns (Fig. 4). Aerobic CH_4 oxidation rates tended to be faster than anaerobic ones, since aerobic CH_4 oxidation consumed on average 0.9 % of initial CH_4 per hour, while anaerobic CH_4 oxidation consumed 0.2 % of initial CH_4 per hour. With molybdate added, 0.2 % of initial CH_4 concentrations were also consumed per hour on average.

The dry season was characterized by higher maximum CH_4 oxidation rates in oxic waters compared to anoxic waters. The maximum oxic and anoxic oxidation rates were observed in August 2014 and were 27 ± 2 (at 55 m) and 16 ± 8 (at 75 m) µmol L^{-1} d^{-1}, respectively. A high SO_4^{2-} consumption rate of 7.5 ± 0.0 µmol L^{-1} d^{-1} was observed near this region of high CH_4 oxidation rate, at 70 m depth. During the other field campaigns, maximum oxic CH_4 oxidation rates were 2 ± 0.04 and 13.9 ± 0.0 µmol L^{-1} d^{-1}, while maximum anoxic rates were 0.8 ± 0.01 (at 47.5 m) and 3.5 ± 0.3 (at 65 m) µmol L^{-1} d^{-1}, in June 2011 and September 2013, respectively. In October 2012, the CH_4 oxidation rate (0.2 µmol L^{-1} d^{-1}) observed in anoxic waters was negligible compared with the high rate of 10.2 ± 0.4 µmol L^{-1} d^{-1} observed in oxic waters. NO_3^- consumption rates tended to be low during all the campaigns, but a non-negligible natural denitrification rate of 1.5 µmol L^{-1} d^{-1} was observed at 65 m in September 2013, in parallel incubations.

During the rainy season, maximum CH_4 oxidation rates in anoxic waters were higher than in oxic waters. In February 2012, the maximum anoxic CH_4 oxidation rate of 7.7 ± 0.4 µmol L^{-1} d^{-1} was observed at 50 m and co-occurred with the maximum NO_3^- consumption rate of 0.4 ± 0.1 µmol L^{-1} d^{-1}. In May 2013, the maximum anoxic CH_4 oxidation rate of 3.2 µmol L^{-1} d^{-1} was observed at 65 m, which was close to a NO_3^- consumption rate of 0.03 ± 0.01 µmol L^{-1} d^{-1} observed at 70 m depth. Also, higher rates of natural denitrification (based on ^{15}N) were observed between 60 and 70 m depth, with a maximum of 0.7 µmol NO_3^- L^{-1} d^{-1} at 60 m depth. No oxic CH_4 oxidation rate was observed in February 2012, while a maximum rate of 1.5 ± 0.2 µmol L^{-1} d^{-1} was observed in May 2013.

When molybdate was added, different profiles were observed. In February 2012 and August 2014, CH_4 oxidation rates decreased when molybdate was added, while rates tended to increase when molybdate was added during the other field campaigns. In October 2012 and May 2013 in particular, CH_4 oxidation rates strongly increased when molybdate was added, from 0 ± 0 to 23 ± 0.4 µmol L^{-1} d^{-1} (at 80m) and from 3 to 18 µmol L^{-1} d^{-1} (at 65 m), respectively. In September 2013, CH_4 oxidation rates increased when molybdate was added up to 11 ± 0.5 µmol L^{-1} d^{-1} at 55 m. In August 2014, the addition of molybdate was also accompanied by a strong increase of dissolved Mn (Mn^{2-}) production rates. NO_3^- consumption rates also tended to increase when molybdate was added during all field campaigns. No dissolved Fe (Fe^{2+}) production was observed with or without molybdate added (data not shown).

CH_4 production was observed in oxic waters during the three sampled campaigns, with rates up to 371 nmol L^{-1} d^{-1} in August 2014 (Fig. 5). For the three campaigns, the highest CH_4 production peaks were located at the basis of the zones with high chlorophyll a content, just above the oxic-anoxic interface.

4. Discussion

High CH_4 oxidation rates were observed in oxic and anoxic waters (maximum 27 ± 2 and 16 ± 8 µmol L^{-1} d^{-1}, respectively). Aerobic CH_4 oxidation rates were sometimes very high when considering the initial CH_4 concentrations (Table 1). For example, the maximum aerobic CH_4 oxidation rate of 27 ± 2 µmol L^{-1} d^{-1} observed at 55 m depth in August 2014 occurred at CH_4 concentrations of 42 ± 2 µmol L^{-1}. However, as shown in Table 1, this rate applied on a period of 24h, and 68 % of the initial CH_4 was consumed after 24h. The same observation is made, for example, in June 2011 (at 42.5 and 45 m), February 2012 (at 50 m) and October 2012 (at 53 m).

A great variability in oxidation rates was observed between the different campaigns. The main pathway of CH_4 oxidation was aerobic in June 2011, October 2012 and September 2013 (dry season) and anaerobic in February 2012 and May 2013 (rainy season) (Table 3). In August 2014, aerobic and anaerobic oxidation rates were quite equivalent. As shown by Figure 6, aerobic oxidation rates tended to depend on the oxygenated layer depth. Aerobic CH_4 oxidation rates tended to be higher when the mixed layer was deeper, as usually observed during the dry season. This observation confirms hypothesis by Roland et al. (2016a) who suggested, based on the seasonal evolution with depth of CH_4 concentrations, that during the dry season, the oxic layer deepens and integrated aerobic CH_4 oxidation on the oxic water column is higher. On the contrary, during the rainy season, the oxic layer is thinner, and a greater amount of CH_4 can be anaerobically oxidized before reaching the oxic part of the water column. While aerobic CH_4 oxidation is probably limited by CH_4 concentrations, AOM is probably limited by the availability of electron acceptors due to competition with more favorable processes (such as heterotrophic denitrification, sulfate reduction etc.). Also episodic fluctuations in water column characteristics influence bacterial communities and small variations in the water column structure may influence the abundance and/or distribution of bacterial communities, and thus contribute to the differences observed. Anyway, the relatively high aerobic and anaerobic CH_4 oxidation rates measured during this study and estimated from ^{13}C-CH_4 production by Morana et al. (2015a) explain the low air-water CH_4 fluxes observed throughout the year in Lake Kivu (Borges et al., 2011;Roland et al., 2016a).

Aerobic and anaerobic CH_4 oxidation rates are also high compared with most other lakes (Table 4). Large differences observed can be easily explained by the different characteristics of the environments, such as vertical structure of the water column, CH_4 concentrations, O_2 and other electron acceptors concentrations, or water temperature. Lake Kivu is a tropical lake, so high water temperatures enhance bacterial activity, contrary to temperate and boreal lakes. Also, the water column of Lake Kivu allows the accumulation of high CH_4 concentrations in anoxic waters, which can slowly diffuse to the oxic compartment, allowing the occurrence of both aerobic and anaerobic CH_4 oxidation. It was presently assumed that all the CH_4 present in the water column of Lake Kivu was produced in anoxic sediments, by acetoclastic and hydrogen reduction methanogenesis (Pasche et al., 2011). However, we show here that a part of CH_4 present in oxic waters can come from aerobic CH_4 production. Aerobic CH_4 production has been recently studied (Bogard et al., 2014;Grossart et al., 2011;Tang et al., 2014;Tang et al., 2016), and different mechanisms have been proposed to explain it, among which a link with

phytoplankton that produces methylated compounds (e.g. dimethylsulfoniopropionate (DMSP)), H_2 or acetate, which could then be used by oxygen tolerant methanogenic bacteria to produce CH_4 (Jarrell, 1985;Angel et al., 2011;Grossart et al., 2011). Alternatively, phytoplankton could directly produce CH_4 itself (Lenhart et al., 2016). During our study, the aerobic CH_4 production peaks were always located at the basis of the zones of high Chlorophyll a content. This location may be due to a spatial coupling between the presence of substrates produced by phytoplankton and the presence of oxygen tolerant methanogenic archaea. İnceoğlu et al. (2015) revealed the presence of methanogenic archaea in the anoxic waters and at the oxic-anoxic interface of Lake Kivu, among which *Methanosarcinales.* Angel et al. (2011) showed that some archaea belonging to *Methanosarcinales* are capable to perform methanogenesis under oxic conditions, at lower rates than in anoxic conditions.

Very high AOM rates observed in Lake Matano compared with Lake Kivu may be explained by higher CH_4 concentrations in anoxic waters and greater concentrations of the highly favorable electron acceptor Fe (Sturm et al., 2016). Pasche et al. (2011) reported lower aerobic and anaerobic CH_4 oxidation rates than those we measured, but their CH_4 oxidation measurements were only made during one field campaign, as although we demonstrated during this study that a great seasonal variability in CH_4 oxidation rates can be observed.

Different depth profile patterns were observed when molybdate, the inhibitor of sulfate-reducing bacteria activity, was added. About half of the measurements gave lower rates with molybdate added, and the other half gave higher rates (Fig. 7). In February 2012 and August 2014, AOM rates were lower with molybdate, suggesting the occurrence of AOM coupled with SO_4^{2-} reduction. Measurement of the SO_4^{2-} consumption rate during the incubations were performed in August 2014. The highest rate of SO_4^{2-} consumption (18 ± 6 µmol L^{-1} d^{-1}) was observed at 70 m, what was close to the higher AOM peak of 16 ± 8 µmol L^{-1} d^{-1} observed at 75 m depth. In terms of stoichiometry, Fig. 8a shows that one AOM peak can be easily explained by the SO_4^{2-} reduction rate, since 1 mole of SO_4^{2-} is needed to oxidize 1 mole of CH_4, according to Eq. (6):

$$(6)\quad CH_4 + SO_4^{2-} \rightarrow HCO_3^- + HS^- + H_2O$$

SO_4^{2-} consumption rates were calculated from the change in time of SO_4^{2-} concentrations measured with the nephelometric method, which might not be precise enough, since the detection limit was 52 µmol L^{-1}. So, due to this high detection limit, we might have missed or underestimated some SO_4^{2-} consumption rates, which could potentially be linked to AOM. Vertical profiles of SO_4^{2-} concentrations, measured by ion chromatography (detection limit of 0.5 µmol L^{-1}), show that SO_4^{2-} is present in enough quantity to explain AOM rates observed, for all campaigns (Table 5).

In February 2012, the maximum AOM peak of 7.7 ± 0.4 µmol L^{-1} d^{-1} co-occurred with the maximum NO_3^- consumption peak of 0.4 ± 0.1 µmol L^{-1} d^{-1}, at 50 m depth, suggesting that a part of AOM might have been due to NO_3^- reduction. NO_3^- consumption rates do not clearly determine if denitrification occurs in Lake Kivu, since the NO_3^- consumption recorded during the incubations might reflect the incorporation of N into the biomass, or reduction to ammonium. However, in a companion paper, we showed that natural denitrification occurred in the Northern Basin in 2011 and 2012, at rates ranging between 1.2 and 2232 nmol NO_3^- L^{-1} d^{-1}, during the same field campaigns, at depths close to those where we observed AOM rates (Roland et al., 2016b). Moreover, in May and September 2013, we also observed natural denitrification rates in parallel incubations, and higher denitrification rates co-occurred with higher AOM rates. Fig. 8b and 8c show AOM rates calculated based on the NO_3^-

consumption rates measured in the incubations and based on natural denitrification rates measured in parallel incubations (only in May and September 2013), respectively, and according to the stoichiometry of Eq. (7), where 8 moles of NO_3^- are needed for 5 moles of CH_4 (Raghoebarsing et al., 2006):

$$(7)\quad 5\ CH_4 + 8\ NO_3^- + 8\ H^+ \rightarrow 5\ CO_2 + 4\ N_2 + 14\ H_2O$$

All AOM rates cannot be solely explained by NO_3^- consumption rates. Even natural denitrification rates are not sufficient to explain AOM rates observed. This discrepancy suggests that NO_3^- is not an important electron acceptor for AOM in Lake Kivu, which is not surprising when considering low natural NO_3^- concentrations. Indeed, the majority of AOM rates observed cannot be explained by the NO_x concentrations (Table 5). Only very low AOM rates can be fully explained by NO_x concentrations. Also, it seems that Fe cycling in the water column of Lake Kivu is not well developed, since while particulate Fe concentrations were up to 15 µmol L^{-1}, dissolved Fe concentrations were very low (Fig. 3), suggesting that Fe reduction is a limited process. While particulate Fe concentrations were high enough to explain up to 100% of the small AOM rates observed (Table 5), dissolved Fe concentrations can only explain up to 24% of the small AOM rates, and only 1-5 % of higher AOM rates, according to Eq. (8) (Beal et al., 2009):

$$(8)\quad CH_4 + 8\ Fe(OH)_3 + 15\ H^+ \rightarrow HCO_3^- + 8\ Fe^{2+} + 21\ H_2O$$

Moreover, in August 2014, no Fe^{2+} production rate was observed in the incubations, without and with molybdate added, which tends to support the low occurrence of Fe reduction in the water column of Lake Kivu. It is thus likely that Fe does not play a significant role for AOM.

MnO_2 and Mn^{2+} concentrations were also measured in May 2013, September 2013 and August 2014 (Fig. 3). AOM can occur with MnO_2 as electron acceptor, and produce Mn^{2+} according to Eq. (9) (Beal et al., 2009):

$$(9)\quad CH_4 + 4\ MnO_2 + 7\ H^+ \rightarrow HCO_3^- + 4\ Mn^{2+} + 5\ H_2O$$

According to this relationship, 1 mole of CH_4 consumes 4 moles of MnO_2 and produces 4 moles of Mn^{2+}. In May 2013 and September 2013, we can see that MnO_2 can fully contribute to AOM at depths near the oxic-anoxic interface (Table 5). At 65 m in May 2013, we can see that MnO_2 can only contribute for 45% of AOM rate. Particulate Mn concentrations were very low compared to dissolved Mn concentrations, with a peak located just above the oxic-anoxic interface, for each campaign. Jones et al. (2011) showed the same profile in Lake Matano, and concluded that Mn is recycled at least 15 times before sedimentation. Mn^{2+} is probably oxidized in presence of small quantities of O_2, precipitates and is directly reduced in anoxic waters. The same profile is probably observed in Lake Kivu, and MnO_2 can thus probably significantly contributes to AOM only at depths close to the oxic-anoxic interface. A significant part of AOM could be due to MnO_2 reduction for each depth if we take into account Mn^{2+} concentrations (Table 5), and considering two hypotheses: 1) All the Mn^{2+} measured at each depth come from the reduction of precipitated MnO_2, and 2) all the Mn^{2+} come from MnO_2 reduction with CH_4. However, these hypotheses are unlikely, since Mn^{2+} present at each depth can come from diffusion from upper depths, and MnO_2 can be reduced by other electron donors than CH_4. Also, for SO_4^{2-} and NO_x, other processes such as SO_4^{2-} reduction with organic matter and heterotrophic denitrification can take place. The percentages of AOM reported in Table 5 and the calculated AOM rates reported in Fig. 7 are thus potential maximum percentages and rates.

Nevertheless, CH_4 has the potential to be the major electron donor in anoxic waters of Lake Kivu based on consideration of the standing stocks and fluxes of carbon. Indeed, CH_4 concentration at 70 m is ~385 µmol L^{-1} which is distinctly higher than typical dissolved organic carbon concentrations of 142 µmol L^{-1} that is very refractory anyway (Morana et al., 2014; 2015b) and particulate organic carbon (POC) concentrations in anoxic waters typically lower than 30 µmol L^{-1} (Morana et al., 2015b). In terms of supply of carbon, the CH_4 vertical flux of 9.4 mmol m^{-2} d^{-1} (Morana et al., 2015a) is also higher compared to the downward flux of POC from the mixed layer of 5.2 ± 1.7 mmol m^{-2} d^{-1} (average value of 24 month-deployment of sediment traps in the Northern Basin from November 2012 to November 2014, unpublished data). This is in general agreement with the high methanotrophic production in Lake Kivu (8.2 – 28.6 mmol m^{-2} d^{-1}) estimated by a parallel study (Morana et al., 2015a).

Considering the very high SO_4^{2-} concentrations compared with other potential electron acceptors (mean of 103, 0.40, 0.42 and 4.9 µmol L^{-1} for SO_4^{2-}, NO_x, particulate Mn and particulate Fe, respectively, at depths where AOM was observed), it is likely that AOM in Lake Kivu is mainly coupled to SO_4^{2-} reduction. Moreover, half of the measurements showed that the inhibition of SRB activity by molybdate induced a decrease of AOM rates. However, the other half of the measurements showed that AOM rates were higher when molybdate was added. These results are surprising and difficult to explain. We firstly considered if we artificially induced aerobic oxidation by injecting molybdate, since the solution was not anoxic. As described in Sect. 2.4, we calculated the impact of O_2 supply for each CH_4 oxidation rate, which was clearly limited, since the median value of relative standard deviations (between rates with molybdate and rates with molybdate if no O_2 was added) was 2.5 %, and thus did not strongly influence CH_4 oxidation rates. Even if a significant artificially-induced aerobic oxidation can be ruled out, the O_2 supply could potentially induce NO_3^-, particulate Fe and Mn production, and thus increase AOM linked to these electron acceptors. However, no increased concentrations of these elements was observed during the incubations with molybdate (data not shown). We were not able to directly measure the SO_4^{2-} concentrations in incubations with molybdate with the nephelometric method, due to a reaction between molybdate and reagents inducing absorbance higher than the maximum absorbance measurable for the specific wavelength. Since HS^- oxidation is very fast (Canfield et al., 2005), it is very likely that the artificially introduced O_2 was directly consumed by this way, and thus that SO_4^{2-} concentrations were higher in incubations with molybdate. However, the increase of AOM in presence of molybdate cannot be due to the increase of SO_4^{2-} concentrations, since molybdate inhibit SO_4^{2-} reduction.

We can thus hypothesize that a modification in competitive relationships among the bacterial community in presence of molybdate, such as a decrease of competition between denitrifying bacteria and/or Mn-reducing bacteria and SRB, would explain the higher NO_3^- consumption rates observed with molybdate added. Also, Mn^{2+} production rates increased with molybdate in August 2014. Competitive relationships for electron donors among bacterial communities have already been observed in literature (e.g. Westermann and Ahring, 1987, Achtnich et al., 1995). In Lake Kivu, it is unlikely that the strong increase in AOM rates was only due to a change in competition between SRB and denitrifying bacteria and/or SRB and Mn-reducing bacteria, since NO_3^- and MnO_2 concentrations are in any way insufficient to be responsible for all AOM rates. However, with the present dataset, this hypothesis cannot be definitively ruled out, and further studies are required to really understand the influence

of molybdate on the bacterial communities. The measurement of the bacterial communities' evolution in the incubations, without and with molybdate added, would be really interesting.

5. Conclusions

We put in evidence a diversified CH_4 cycle, with the occurrence of AOM and aerobic CH_4 production, and their seasonal variability, in the water column of a meromictic tropical lake. Presently, CH_4 oxidation in Lake Kivu was superficially measured by Jannasch (1975), and was estimated on the base on mass balance and comparison to fluxes (Pasche et al., 2011;Borges et al., 2011). It was also supposed to occur based on pyrosequencing results (İnceoğlu et al., 2015;Zigah et al., 2015), which put in evidence the presence of sulfate-reducing bacteria and methanotrophic archaea in the water column and suggested that AOM could be coupled to SO_4^{2-} reduction. Morana et al. (2015a) made isotopic composition analysis which revealed the occurrence of aerobic and anaerobic CH_4 oxidation in the water column of Lake Kivu, and concluded that aerobic CH_4 oxidation was probably the main pathway of CH_4 removal. Finally, important CH_4 oxidation was also supposed to be responsible for small CH_4 fluxes to the atmosphere observed throughout the year (Borges et al. 2011; Roland et al., 2016a). However, any of these studies directly put in evidence and measured aerobic and anaerobic oxidation rates and, nothing was known about seasonal and spatial variability of CH_4 oxidation in Lake Kivu, nor the different potential electron acceptors for AOM. We were not able to clearly identify the main electron acceptor of AOM based on this dataset, but considering the high SO_4^{2-} concentrations, it is likely that AOM could be mainly coupled to SO_4^{2-} reduction. A seasonal variability in the respective importance of aerobic and anaerobic CH_4 oxidation rates was observed, with a higher importance of aerobic oxidation in dry season and of AOM in rainy season. This can be linked to the position of the oxygenated layer depth, which is located deeper during the dry season, due to the seasonal mixing of the mixolimnion. At this period of the year, the oxic-anoxic interface is located close to the chemocline, below which the CH_4 concentrations are typically 5 orders of magnitude larger than in the upper part of the mixolimnion. By contrast, during the rainy season, when the thermal stratification within the mixolimnion is well established, the volume of the oxic compartment is smaller than the volume of the anoxic compartment, and hence CH_4 can only reach the oxic waters by diffusion, after that a significant fraction of the CH_4 upward flux has been oxidized by AOM, which limit the aerobic CH_4 oxidation.

Author contributions

FAER, FD and AVB designed the experiments. FAER and AVB were responsible for manuscript preparation. FAER was also responsible for the fieldwork, the data acquisition, analysis and interpretation.

CM, FD, SC participated in fieldwork. CM, FD, SC and BT were involved in scientific discussions, data interpretation and manuscript preparation. SC was also involved in measurements of nutrients, sulfate and sulfide concentrations. BT also organized denitrification, nutrients, sulfate and sulfide measurements in the Institute of Biology and Nordic Center for Earth Evolution (University of Southern Denmark).

Acknowledgements

We thank the Rwanda Energy Company for the access to their platform for the sampling, Renzo Biondo (University of Liège), Laura Bristow, Dina Holmgaard Skov and Heidi Grøn Jensen (University of Southern Denmark) for help in measurements. This study was funded by the Belgian Federal Science Policy Office (BELSPO, Belgium) under the EAGLES (East African Great lake Ecosystem Sensitivity to Changes, SD/AR/02A) project, by the Fonds National de la Recherche Scientifique (FNRS) under the MICKI (Microbial diversity and processes in Lake Kivu, 1715859) project, and contributes to the European Research Council (ERC) starting grant project AFRIVAL (African river basins: Catchment-scale carbon fluxes and transformations, 240002). GC was acquired with funds from the FNRS (contract n°2.4.598.07). AVB is a senior research associate at the FNRS. FAER has a PhD grant from FNRS (« Fonds pour la formation à la Recherche dans l'Industrie et dans l'Agriculture » - FRIA).

References

á Norði, K., Thamdrup, B., and Schubert, C. J.: Anaerobic oxidation of methane in an iron-rich Danish freshwater lake sediment, Limnol. Oceanogr., 58, 546-554, doi:10.4319/lo.2013.58.2.0546, 2013.

á Norði, K., and Thamdrup, B.: Nitrate-dependent anaerobic methane oxidation in a freshwater sediment, Geochim. Cosmochim. Acta, 132, 141-150, doi:10.1016/j.gca.2014.01.032, 2014.

Achtnich, C., Bak, F., and Conrad, R.: Competition for electron donors among nitrate reducers, ferric iron reducers, sulfate reducers, and methanogens in anoxic paddy soil, Biol Fert Soils, 19, 65-72, doi:10.1007/BF00336349, 1995.

Angel, R., Matthies, D., and Conrad, R.: Activation of Methanogenesis in Arid Biological Soil Crusts Despite the Presence of Oxygen, PLoS ONE, 6, e20453, 10.1371/journal.pone.0020453, 2011.

APHA: Standard methods for the examination of water and wastewater, edited by: APHA, Washington, 1998.

Bastviken, D., Ejlertsson, J., and Tranvik, L.: Measurement of methane oxidation in lakes: A comparison of methods, Environ. Sci. Technol., 36, 3354-3361, doi:10.1021/es010311p, 2002.

Bastviken, D., Tranvik, L. J., Downing, J. A., Crill, P. M., and Enrich-Prast, A.: Freshwater methane emissions offset the continental carbon sink, Science, 331, 50, doi:10.1126/science.1196808, 2011.

Beal, E. J., House, C. H., and Orphan, V. J.: Manganese-and iron-dependent marine methane oxidation, Science, 325, 184-187, doi:10.1126/science.1169984, 2009.

Boetius, A., Ravenschlag, K., Schubert, C. J., Rickert, D., Widdel, F., Gieseke, A., Amann, R., Jørgensen, B. B., Witte, U., and Pfannkuche, O.: A marine microbial consortium apparently mediating anaerobic oxidation of methane, Nature, 407, 623-626, doi:10.1038/35036572, 2000.

Bogard, M. J., del Giorgio, P. A., Boutet, L., Chaves, M. C. G., Prairie, Y. T., Merante, A., and Derry, A. M.: Oxic water column methanogenesis as a major component of aquatic CH4 fluxes, Nat. Commun., 5, doi:10.1038/ncomms6350, 2014.

Borges, A. V., Abril, G., Delille, B., Descy, J. P., and Darchambeau, F.: Diffusive methane emissions to the atmosphere from Lake Kivu (Eastern Africa), J. Geophys. Res. Biogeosci., 116, doi:10.1029/2011JG001673, 2011.

Borges, A. V., Darchambeau, F., Teodoru, C. R., Marwick, T. R., Tamooh, F., Geeraert, N., Omengo, F. O., Guérin, F., Lambert, T., and Morana, C.: Globally significant greenhouse-gas emissions from African inland waters, Nat. Geosci., 8, 637-642, doi:10.1038/ngeo2486, 2015.

Borrel, G., Jézéquel, D., Biderre-Petit, C., Morel-Desrosiers, N., Morel, J.-P., Peyret, P., Fonty, G., and Lehours, A.-C.: Production and consumption of methane in freshwater lake ecosystems, Res. Microbiol., 162, 832-847, doi:10.1016/j.resmic.2011.06.004, 2011.

Braman, R. S., and Hendrix, S. A.: Nanogram nitrite and nitrate determination in environmental and biological materials by vanadium(III) reduction with chemiluminescence detection, Anal. Chem., 61, 2715-2718, doi:10.1021/ac00199a007, 1989.

Canfield, D. E., Kristensen, E., and Thamdrup, B.: The sulfur cycle, Adv. Mar. Biol., 48, 313-381, doi:10.1016/S0065-2881(05)48009-8, 2005.

Cline, J. D.: Spectrophotometric determination of hydrogen sulfide in natural waters, Limnol. Oceanogr., 14, 454-458, doi:10.4319/lo.1969.14.3.0454, 1969.

Conrad, R.: The global methane cycle: Recent advances in understanding the microbial processes involved, Environ. Microbiol. Rep., 1, 285-292, doi:10.1111/j.1758-2229.2009.00038.x, 2009.

Crowe, S., Katsev, S., Leslie, K., Sturm, A., Magen, C., Nomosatryo, S., Pack, M., Kessler, J., Reeburgh, W., and Roberts, J.: The methane cycle in ferruginous Lake Matano, Geobiol., 9, 61-78, doi:10.1111/j.1472-4669.2010.00257.x, 2011.

Cui, M., Ma, A., Qi, H., Zhuang, X., and Zhuang, G.: Anaerobic oxidation of methane: an "active" microbial process, Microbiologyopen, 4, 1-11, doi:10.1002/mbo3.232, 2015.

Ettwig, K. F., Butler, M. K., Le Paslier, D., Pelletier, E., Mangenot, S., Kuypers, M. M., Schreiber, F., Dutilh, B. E., Zedelius, J., and De Beer, D.: Nitrite-driven anaerobic methane oxidation by oxygenic bacteria, Nature, 464, 543-548, 2010.

Grossart, H.-P., Frindte, K., Dziallas, C., Eckert, W., and Tang, K. W.: Microbial methane production in oxygenated water column of an oligotrophic lake, PNAS, 108, 19657-19661, 10.1073/pnas.1110716108, 2011.

Haroon, M. F., Hu, S., Shi, Y., Imelfort, M., Keller, J., Hugenholtz, P., Yuan, Z., and Tyson, G. W.: Anaerobic oxidation of methane coupled to nitrate reduction in a novel archaeal lineage, Nature, 500, 567-570, 2013.

Hu, S., Zeng, R. J., Keller, J., Lant, P. A., and Yuan, Z.: Effect of nitrate and nitrite on the selection of microorganisms in the denitrifying anaerobic methane oxidation process, Environ. Microbiol. Rep., 3, 315-319, 2011.

İnceoğlu, Ö., Llirós, M., García-Armisen, T., Crowe, S. A., Michiels, C., Darchambeau, F., Descy, J.-P., and Servais, P.: Distribution of bacteria and archaea in meromictic tropical Lake Kivu (Africa), Aquat. Microb. Ecol., 74, 215-233, doi:10.3354/ame01737, 2015.

Iversen, N., and Jørgensen, B.: Anaerobic methane oxidation rates at the sulfate-methane transition in marine sediments from Kattegat and Skagerrak (Denmark), Limnol. Oceanogr., 30, 944-955, doi:10.4319/lo.1985.30.5.0944, 1985.

Iversen, N., Oremland, R. S., and Klug, M. J.: Big Soda Lake (Nevada). 3. Pelagic methanogenesis and anaerobic methane oxidation, Limnol. Oceanogr., 32, 804-814, doi:10.4319/lo.1987.32.4.0804, 1987.

Jannasch, H. W.: Methane oxidation in Lake Kivu (central Africa)1, Limnol. Oceanogr., 20, 860-864, doi:10.4319/lo.1975.20.5.0860, 1975.

Jarrell, K. F.: Extreme Oxygen Sensitivity in Methanogenic Archaebacteria, Bioscience, 35, 298-302, doi:10.2307/1309929, 1985.

Jones, C., Crowe, S. A., Sturm, A., Leslie, K. L., MacLean, L. C. W., Katsev, S., Henny, C., Fowle, D. A., and Canfield, D. E.: Biogeochemistry of manganese in ferruginous Lake Matano, Indonesia, Biogeosciences, 8, 2977-2991, doi:10.5194/bg-8-2977-2011, 2011.

Jørgensen, B. B., Weber, A., and Zopfi, J.: Sulfate reduction and anaerobic methane oxidation in Black Sea sediments, Deep-Sea Res. Pt. I, 48, 2097-2120, doi:10.1016/S0967-0637(01)00007-3, 2001.

Kirschke, S., Bousquet, P., Ciais, P., Saunois, M., Canadell, J. G., Dlugokencky, E. J., Bergamaschi, P., Bergmann, D., Blake, D. R., Bruhwiler, L., Cameron-Smith, P., Castaldi, S., Chevallier, F., Feng, L., Fraser, A., Heimann, M., Hodson, E. L., Houweling, S., Josse, B., Fraser, P. J., Krummel, P. B., Lamarque, J. F., Langenfelds, R. L., Le Quéré, C., Naik, V., O'Doherty, S., Palmer, P. I., Pison, I., Plummer, D., Poulter, B., Prinn, R. G., Rigby, M., Ringeval, B., Santini, M., Schmidt, M., Shindell, D. T., Simpson, I. J., Spahni, R., Steele, L. P., Strode, S. A., Sudo, K., Szopa, S., Van Der Werf, G. R., Voulgarakis, A., Van Weele, M., Weiss, R. F., Williams, J. E., and Zeng, G.: Three decades of global methane sources and sinks, Nat. Geosci., 6, 813-823, doi:10.1038/ngeo1955, 2013.

Lenhart, K., Klintzsch, T., Langer, G., Nehrke, G., Bunge, M., Schnell, S., and Keppler, F.: Evidence for methane production by the marine algae Emiliania huxleyi, Biogeosciences, 13, 3163-3174, doi:10.5194/bg-13-3163-2016, 2016.

Lopes, F., Viollier, E., Thiam, A., Michard, G., Abril, G., Groleau, A., Prévot, F., Carrias, J.-F., Albéric, P., and Jézéquel, D.: Biogeochemical modelling of anaerobic vs. aerobic methane oxidation in a meromictic crater lake (Lake Pavin, France), Appl. Geochem., 26, 1919-1932, doi:10.1016/j.apgeochem.2011.06.021, 2011.

Miranda, K. M., Espey, M. G., and Wink, D. A.: A rapid, simple spectrophotometric method for simultaneous detection of nitrate and nitrite, Nitric Oxide-Biol. Ch., 5, 62-71, doi:10.1006/niox.2000.0319, 2001.

Morana, C., Sarmento, H., Descy, J. P., Gasol, J. M., Borges, A. V., Bouillon, S., and Darchambeau, F.: Production of dissolved organic matter by phytoplankton and its uptake by heterotrophic prokaryotes in large tropical lakes, Limnol. Oceanogr., 59, 1364-1375, doi:10.4319/lo.2014.59.4.1364, 2014.

Morana, C., Borges, A. V., Roland, F. A. E., Darchambeau, F., Descy, J. P., and Bouillon, S.: Methanotrophy within the water column of a large meromictic tropical lake (Lake Kivu, East Africa), Biogeosciences, 12, 2077-2088, doi:10.5194/bg-12-2077-2015, 2015a.

Morana, C., Darchambeau, F., Roland, F. A. E., Borges, A. V., Muvundja, F. A., Kelemen, Z., Masilya, P., Descy, J. P., and Bouillon, S.: Biogeochemistry of a large and deep tropical lake (Lake Kivu, East Africa): insights from a stable isotope study covering an annual cycle, Biogeosciences, 12, 4953-4963, doi:10.5194/bg-12-4953-2015, 2015b.

Morana, C., Roland, F. A., Crowe, S. A., Llirós, M., Borges, A. V., Darchambeau, F., and Bouillon, S.: Chemoautotrophy and anoxygenic photosynthesis within the water column of a large meromictic tropical lake (Lake Kivu, East Africa), Limnol. Oceanogr., doi:10.1002/lno.10304, 2016.

Nisbet, E. G., Dlugokencky, E. J., Manning, M. R., Lowry, D., Fisher, R. E., France, J. L., Michel, S. E., Miller, J. B., White, J. W. C., Vaughn, B., Bousquet, P., Pyle, J. A., Warwick, N. J., Cain, M., Brownlow, R., Zazzeri, G., Lanoisellé, M., Manning, A. C., Gloor, E., Worthy, D. E. J., Brunke, E. G., Labuschagne, C., Wolff, E. W., and Ganesan, A. L.: Rising atmospheric methane: 2007–2014 growth and isotopic shift, Glob. Biogeochem. Cycles, 30, 1356-1370, doi:10.1002/2016GB005406, 2016.

Pasche, N., Schmid, M., Vazquez, F., Schubert, C. J., Wüest, A., Kessler, J. D., Pack, M. A., Reeburgh, W. S., and Bürgmann, H.: Methane sources and sinks in Lake Kivu, J. Geophys. Res. Biogeosci., 116, G03006, doi:10.1029/2011JG001690, 2011.

Raghoebarsing, A. A., Pol, A., Van de Pas-Schoonen, K. T., Smolders, A. J., Ettwig, K. F., Rijpstra, W. I. C., Schouten, S., Damsté, J. S. S., den Camp, H. J. O., and Jetten, M. S.: A microbial consortium couples anaerobic methane oxidation to denitrification, Nature, 440, 918-921, doi:10.1038/nature04617, 2006.

Rodier, J., Bazin, C., Broutin, J., Chambon, P., Champsaur, H., and Rodi, L.: L'Analyse de l'Eau (8ème édn), Dunod, Paris: France, 1996.

Roland, F. A. E., Darchambeau, F., Morana, C., and Borges, A. V.: Nitrous oxide and methane seasonal variability in the epilimnion of a large tropical meromictic lake (Lake Kivu, East-Africa), Aquat. Sci., 1-10, doi:10.1007/s00027-016-0491-2, 2016a.

Roland, F. A. E., Crowe, S., Borges, A. V., De Brabandere, L., Morana, C., Servais, P., Thamdrup, B., and Darchambeau, F.: Denitrification, anaerobic ammonium oxidation and dissimilatory nitrate reduction to ammonium in an East African Great Lake (Lake Kivu), Limnol. Oceanogr., (in prep), 2016b.

Rudd, J. W.: Methane oxidation in Lake Tanganyika (East Africa), Limnol. Oceanogr., 25, 958-963, doi:10.4319/lo.1980.25.5.0958, 1980.

Rudd, J. W. M., Hamilton, R. D., and Campbell, N. E. R.: Measurement of microbial oxidation of methane in lake water, Limnol. Oceanogr., 19, 519-524, doi:10.4319/lo.1974.19.3.0519, 1974.

Sarmento, H., Isumbisho, M., and Descy, J.-P.: Phytoplankton ecology of Lake Kivu (eastern Africa), J. Plankton Res., 28, 815-829, 2006.

Saunois, M., Bousquet, P., Poulter, B., Peregon, A., Ciais, P., Canadell, J. G., Dlugokencky, E. J., Etiope, G., Bastviken, D., Houweling, S., Janssens-Maenhout, G., Tubiello, F. N., Castaldi, S., Jackson, R. B., Alexe, M., Arora, V. K., Beerling, D. J., Bergamaschi, P., Blake, D. R., Brailsford, G., Brovkin, V., Bruhwiler, L., Crevoisier, C., Crill, P., Curry, C., Frankenberg, C., Gedney, N., Höglund-Isaksson, L., Ishizawa, M., Ito, A., Joos, F., Kim, H. S., Kleinen, T., Krummel, P., Lamarque, J. F., Langenfelds, R., Locatelli, R., Machida, T., Maksyutov, S., McDonald, K. C., Marshall, J., Melton, J. R., Morino, I., O'Doherty, S., Parmentier, F. J. W., Patra, P. K., Peng, C., Peng, S., Peters, G. P., Pison, I., Prigent, C., Prinn, R., Ramonet, M., Riley, W. J., Saito, M., Schroeder, R., Simpson, I. J., Spahni, R., Steele, P., Takizawa, A., Thornton, B. F., Tian, H., Tohjima, Y., Viovy, N., Voulgarakis, A., van Weele, M., van der Werf, G., Weiss, R., Wiedinmyer, C., Wilton, D. J., Wiltshire, A., Worthy, D., Wunch, D. B., Xu, X., Yoshida, Y., Zhang, B., Zhang, Z., and Zhu, Q.: The Global Methane Budget: 2000-2012, Earth Syst. Sci. Data Discuss., 2016, 1-79, doi:10.5194/essd-2016-25, 2016.

Schubert, C. J., Lucas, F., Durisch-Kaiser, E., Stierli, R., Diem, T., Scheidegger, O., Vazquez, F., and Müller, B.: Oxidation and emission of methane in a monomictic lake (Rotsee, Switzerland), Aquat sci, 72, 455-466, 2010.

Sivan, O., Adler, M., Pearson, A., Gelman, F., Bar-Or, I., John, S. G., and Eckert, W.: Geochemical evidence for iron-mediated anaerobic oxidation of methane, Limnol. Oceanogr., 56, 1536-1544, 2011.

Sturm, A., Fowle, D. A., Jones, C., Leslie, K., Nomosatryo, S., Henny, C., Canfield, D. E., and Crowe, S. A.: Rates and pathways of CH4 oxidation in ferruginous Lake Matano, Indonesia, Biogeosciences Discuss., 2016, 1-34, doi:10.5194/bg-2015-533, 2016.

Tang, K. W., McGinnis, D. F., Frindte, K., Brüchert, V., and Grossart, H.-P.: Paradox reconsidered: Methane oversaturation in well-oxygenated lake waters, Limnol. Oceanogr., 59, 275-284, doi:10.4319/lo.2014.59.1.0275, 2014.

Tang, K. W., McGinnis, D. F., Ionescu, D., and Grossart, H.-P.: Methane Production in Oxic Lake Waters Potentially Increases Aquatic Methane Flux to Air, Environ. Sci. Technol. Lett., 3, 227-233, doi:10.1021/acs.estlett.6b00150, 2016.

Thamdrup, B., and Dalsgaard, T.: Production of N2 through anaerobic ammonium oxidation coupled to nitrate reduction in marine sediments, Appl. Environ. Microbiol., 68, 1312-1318, doi:10.1128/AEM.68.3, 2002.

Weiss, R. F., and Price, B. A.: Nitrous oxide solubility in water and seawater, Mar. Chem., 8, 347-359, doi:10.1016/0304-4203(80)90024-9, 1980.

Weiss, R. F.: Determinations of carbon dioxide and methane by dual catalyst flame ionization chromatography and nitrous oxide by electron capture chromatography, J. Chromatogr. Sci., 19, 611-616, doi:10.1093/chromsci/19.12.611, 1981.

Westermann, P., and Ahring, B. K.: Dynamics of methane production, sulfate reduction, and denitrification in a permanently waterlogged alder swamp, Appl. Environ. Microbiol., 53, 2554-2559, 1987.

Yamamoto, S., Alcauskas, J. B., and Crozier, T. E.: Solubility of methane in distilled water and seawater, J. Chem. Eng. Data, 21, 78-80, doi:10.1021/je60068a029, 1976.

Zigah, P. K., Oswald, K., Brand, A., Dinkel, C., Wehrli, B., and Schubert, C. J.: Methane oxidation pathways and associated methanotrophic communities in the water column of a tropical lake, Limnol. Oceanogr., 60, 553-572, doi:10.1002/lno.10035, 2015.

Table 1: Depth (m) where CH_4 oxidation was observed, presence (+) or absence (-) of oxygen (O_2), CH_4 oxi = maximum CH_4 oxidation rates (µmol L^{-1} d^{-1}) calculated based on a linear regression, $[CH_4]_{in}$ = initial CH_4 concentrations (µmol L^{-1}) from which the linear regression begins, % CH_4 = percentage of initial CH_4 consumed, and time (h) required for this consumption (time lapse during which the linear regression was applied to calculate CH_4 oxidation rates), without and with molybdate added (- Mo and + Mo, respectively), for all field campaigns. N.d. = not determined.

Depth (m)	**O_2**	**CH_4 oxi (µmol L^{-1} d^{-1})**		**$[CH_4]_{in}$ (µmol L^{-1})**		**% CH_4**		**Time (h)**	
		- Mo	**+ Mo**	**- Mo**	**+ Mo**	**- Mo**	**+ Mo**	**- Mo**	**+ Mo**
				June 2011					
42.5	+	0.3 ± 0.0	N.d.	0.3 ± 0	N.d.	90 ± 0	N.d.	24	N.d.
45	+	2.0 ± 0.0	N.d.	2 ± 0	N.d.	97 ± 0	N.d.	24	N.d.
47.5	-	0.8 ± 0.0	N.d.	18 ± 0	N.d.	23 ± 0	N.d.	96	N.d.
50	-	0.4 ± 0.1	N.d.	21 ± 0	N.d.	10 ± 0	N.d.	96	N.d.
				February 2012					
45	-	0.3 ± 0.0	0.1 ± 0.0	1 ± 0	1 ± 0	73 ± 0	66 ± 0	72	72
50	-	7.7 ± 0.4	3.0 ± 0.3	8 ± 0	8 ± 0	64 ± 1	27 ± 2	16	16
55	-	4.0 ± 0.2	4.3 ± 0.0	21 ± 0	21 ± 0	12 ± 1	13 ± 0	16	16
60	-	1.2	0.2	115	105	4	3	72	96
				October 2012					
53	+	10.2 ± 0.4	10.0 ± 0.4	10 ± 0	10 ± 0	98 ± 0	97 ± 0	24	24
55	+	0.4 ± 0.4	16.9 ± 5.4	78 ± 4	78 ± 4	2 ± 6	18 ± 5	96	24
57.5	-	0.2 ± 0.2	1.3 ± 0.5	65 ± 3	65 ± 3	4 ± 5	10 ± 5	96	96
60	-	0.0 ± 0.0	2.1 ± 2.5	129 ± 17	129 ± 17	0 ± 0	10 ± 12	96	96
70	-	0.0 ± 0.0	1.3 ± 1.6	344 ± 11	344 ± 11	0 ± 0	2 ± 3	96	96
80	-	0.0 ± 0.0	23.4 ± 0.4	538 ± 2	538 ± 2	0 ± 0	26 ± 0	96	96
				May 2013					
40	+	0.1 ± 0.0	N.d.	0.4 ± 0	N.d.	45 ± 2	N.d.	96	N.d.
45	+	0.1 ± 0.0	N.d.	0.7 ± 0	N.d.	63 ± 1	N.d.	72	N.d.
47.5	+	0.6 ± 0.0	0.6 ± 0.0	2 ± 0	2 ± 0	75 ± 1	75 ± 1	48	48
50	+	1.5 ± 0.2	1.0 ± 0.3	20 ± 1	20 ± 1	31 ± 4	18 ± 5	96	72
52.5	+	0.5 ± 0.1	0.3 ± 0.0	25 ± 0	25 ± 0	7 ± 1	7 ± 1	72	96
55	-	1.2	4.5 ± 4.2	45	45 ± 4	8	8 ± 7	96	24
60	-	1.0	6.0 ± 5.6	115	113 ± 4	4	4 ± 4	96	24
65	-	3.2	18.0	227	223	6	6	96	24
70	-	1.5 ± 0.3	1.0 ± 0.0	410 ± 3	410 ± 3	2 ± 1	2 ± 1	120	120
				September 2013					
40	+	0.02	N.d.	0.2	N.d.	37	N.d.	48	N.d.
45	+	0.02 ± 0.0	0.0 ± 0.0	0.1 ± 0	0.1 ± 0	73 ± 3	0 ± 0	96	96

47.5	+	13.4 ± 0.3	10.5 ± 0.3	13 ± 0	13 ± 0	93 ± 0	75 ± 1	24	24
50	+	13.9 ± 0.0	12.7 ± 0.0	27 ± 0	27 ± 0	17 ± 0	16 ± 0	12	12
52.5	+	0.2 ± 0.0	1.0 ± 0.0	50 ± 0	50 ± 0	2 ± 0	11 ± 0	96	96
55	-	0.5 ± 0.0	11.3 ± 0.5	90 ± 0	90 ± 0	2 ± 0	4 ± 0	72	12
57.5	-	0.3 ± 0.0	10.2 ± 0.4	99 ± 0	99 ± 0	3 ± 0	3 ± 0	96	12
65	-	3.5 ± 0.3	2.6 ± 0.3	215 ± 1	215 ± 1	6 ± 1	5 ± 1	72	72
				August 2014					
55	+	27.1 ± 1.6	18.0 ± 1.6	42 ± 2	42 ± 2	68 ± 1	46 ± 3	24	24
57.5	+	2.1	1.5	69	69	6	4	48	48
60	-	0.0 ± 0.0	4.7	167 ± 20	167 ± 20	0 ± 0	6	96	48
65	-	5.1 ± 0.9	1.3 ± 0.9	275 ± 1	275 ± 1	6 ± 2	3 ± 2	96	96
67.5	-	6.8 ± 7.8	0.0 ± 0.0	358 ± 6	358 ± 6	16 ± 12	0 ± 0	96	96
70	-	3.3 ± 1.3	0.0 ± 0.0	445 ± 10	445 ± 10	6 ± 2	0 ± 0	96	96
75	-	16.0 ± 8.2	0.0 ± 0.0	689 ± 58	689 ± 58	3 ± 8	0 ± 0	96	96

Table 2: Anoxic depths (m), NO_3^- and SO_4^{2-} consumption and Mn^{2+} production rates (µmol L^{-1} d^{-1}) and their standard deviation, without and with molybdate added (- Mo and + Mo, respectively), for all campaigns. N.d. = not determined. All rates were calculated based on a linear regression of concentrations through time. Fe^{2+} production rates were measured at the same depths than Mn^{2+} production rates, but were always equal to zero and are not reported here.

Depth (m)	NO_3^- consumption (µmol L^{-1} d^{-1})		SO_4^{2-} consumption (µmol L^{-1} d^{-1})		Mn^{2+} production (µmol L^{-1} d^{-1})	
	- Mo	**+ Mo**	**- Mo**	**+ Mo**	**- Mo**	**+ Mo**
February 2012						
45	0.01 ± 0.01	0.0 ± 0.0	N.d.	N.d.	N.d.	N.d.
50	0.37 ± 0.07	0.56 ± 0.02	N.d.	N.d.	N.d.	N.d.
55	0.21 ± 0.02	0.0 ± 0.0	N.d.	N.d.	N.d.	N.d.
60	0.01 ± 0.0	0.33 ± 0.0	N.d.	N.d.	N.d.	N.d.
October 2012						
57.5	0.0 ± 0.0	0.0 ± 0.0	N.d.	N.d.	N.d.	N.d.
60	0.0	0.02	N.d.	N.d.	N.d.	N.d.
65	0.0	0.04	N.d.	N.d.	N.d.	N.d.
70	0.0	0.04	N.d.	N.d.	N.d.	N.d.
May 2013						
55	0.0 ± 0.0	0.0 ± 0.0	N.d.	N.d.	N.d.	N.d.
60	0.07	0.0	N.d.	N.d.	N.d.	N.d.
65	0.0 ± 0.0	0.0 ± 0.0	N.d.	N.d.	N.d.	N.d.
70	0.03 ± 0.01	0.25 ± 0.05	N.d.	N.d.	N.d.	N.d.
September 2013						
55	0.0 ± 0.0	0.0 ± 0.0	N.d.	N.d.	N.d.	N.d.
57.5	0.0 ± 0.0	0.0 ± 0.0	N.d.	N.d.	N.d.	N.d.
65	0.0 ± 0.0	0.04 ± 0.01	N.d.	N.d.	N.d.	N.d.
August 2014						
60	0.0 ± 0.0	0.0 ± 0.0	1.0 ± 0.5	N.d.	0.0 ± 0.0	0.0 ± 0.0
62.5	0.0 ± 0.0	0.0 ± 0.0	0.7 ± 0.3	N.d.	0.0 ± 0.0	0.5 ± 0.2
65	0.0 ± 0.0	0.0 ± 0.0	0.0 ± 0.0	N.d.	0.0 ± 0.0	0.0 ± 0.0
67.5	0.0 ± 0.0	0.0 ± 0.0	1.5 ± 0.6	N.d.	0.0 ± 0.0	10.6 ± 1.6
70	0.0 ± 0.0	0.0 ± 0.0	7.5 ± 0.0	N.d.	0.0 ± 0.0	8.1 ± 0.1
75	0.0 ± 0.0	0.0 ± 0.0	0.3 ± 0.03	N.d.	0.0 ± 0.0	0.0 ± 0.0

Table 3: Depth-integrated CH_4 oxidation rates (µmol m^{-2} d^{-1}) in Lake Kivu and the percent related to anaerobic oxidation of methane (AOM).

	Integration depth interval (m)	**CH_4 oxidation (µmol m^{-2} d^{-1})**	**% AOM**
	Dry season		
June 2011	1-65	9	30
October 2012	1-80	27	1
September 2013	1-65	81	15
August 2014	1-75	162	55
	Rainy season		
February 2012	1-60	63	99
May 2013	1-80	44	81

Table 4: Aerobic and anaerobic CH_4 oxidation rates (µmol L^{-1} d^{-1}) in Lake Kivu and other lakes in literature.

Lake	Aerobic CH_4 oxidation (µmol L^{-1} d^{-1}) (CH_4 concentrations; µmol L^{-1})	AOM (µmol L^{-1} d^{-1}) (CH_4 concentrations; µmol L^{-1})	Source
Kivu	0.02-27 (0.2-42)	0.2-16 (65-689)	This study
Kivu	0.62 (3.6)	1.1 (54)	Pasche et al. (2011)
Pavin (France)	0.006-0.046 (0.06-0.35)	0.4 (285-785)	Lopes et al. (2011)
Big Soda (US)	0.0013 (0.1)	0.060 (50)	Iversen et al. (1987)
Marn (Sweden)	0.8 (10)	2.2 (55)	Bastviken et al. (2002)
Tanganyika	0.1-0.96 (<10)	0.24-1.8 (~10)	Rudd (1980)
Matano (Indonesia)	0.00036-0.0025 (0.5)	4.2-117 (12-484)	Sturm et al. (2016)

Table 5: SO_4^{2-}, NO_x, Mn^{2+}, MnO_2, Fe^{2+} and $Fe(OH)_3$ concentrations (µmol L^{-1}) and potential anaerobic CH_4 oxidation (%) based on these concentrations for all campaigns, for each depth where AOM rates were observed. N.d. = not determined.

Field campaign	Depth (m)	$[SO_4^{2-}]$ (µmol L^{-1}) (%)	$[NO_x]$ (µmol L^{-1}) (%)	$[Mn^{2+}]$ (µmol L^{-1}) (%)	$[MnO_2]$ (µmol L^{-1}) (%)	$[Fe^{2+}]$ (µmol L^{-1}) (%)	$[Fe(OH)_3]$ (µmol L^{-1}) (%)
June 2011	47.5	125.6 (100)	0.23 (18)	N.d.	N.d.	N.d.	N.d.
	50	158.8 (100)	0.24 (38)	N.d.	N.d.	N.d.	N.d.
February 2012	45	168.5 (100)	1.84 (100)	N.d.	N.d.	N.d.	N.d.
	47.5	160.9 (100)	1.08 (9)	N.d.	N.d.	N.d.	N.d.
	50	108.4 (100)	0.04 (1)	N.d.	N.d.	N.d.	N.d.
	55	77.0 (100)	0.38 (20)	N.d.	N.d.	N.d.	N.d.
October 2012	57.5	N.d.	0.53 (100)	N.d.	N.d.	N.d.	N.d.
May 2013	55	130.4 (100)	0.04 (2)	3.0 (63)	0.2 (100)	0.1 (1)	4.8 (50)
	60	135.4 (100)	0.15 (9)	5.5 (100)	0.2 (100)	1.3 (17)	4.9 (61)
	65	112.2 (100)	0.11 (2)	7.3 (57)	0.2 (45)	1.3 (5)	4.7 (18)
	70	47.5 (100)	0.2 (8)	8.0 (100)	N.d.	1.3 (11)	N.d.
September 2013	55	130.5 (100)	0.91 (100)	8.7 (100)	0.7 (100)	0.3 (8)	4.9 (100)
	57.5	124.1 (100)	0.43 (90)	9.2 (100)	0.8 (100)	0.6 (24)	5.4 (100)
	60	108.1 (100)	0.43 (8)	9.5 (68)	N.d.	0.9 (3)	N.d.
August 2014	65	60.6 (100)	0.20 (2)	8.8 (43)	N.d.	1.1 (3)	N.d.
	67.5	45.5 (100)	0.00 (0)	9.2 (34)	N.d.	2.2 (4)	N.d.
	70	25.6 (100)	0.33 (6)	9.3 (70)	N.d.	1.1 (4)	N.d.
	75	10.7 (67)	0.13 (1)	9.4 (15)	N.d.	0.7 (1)	N.d.

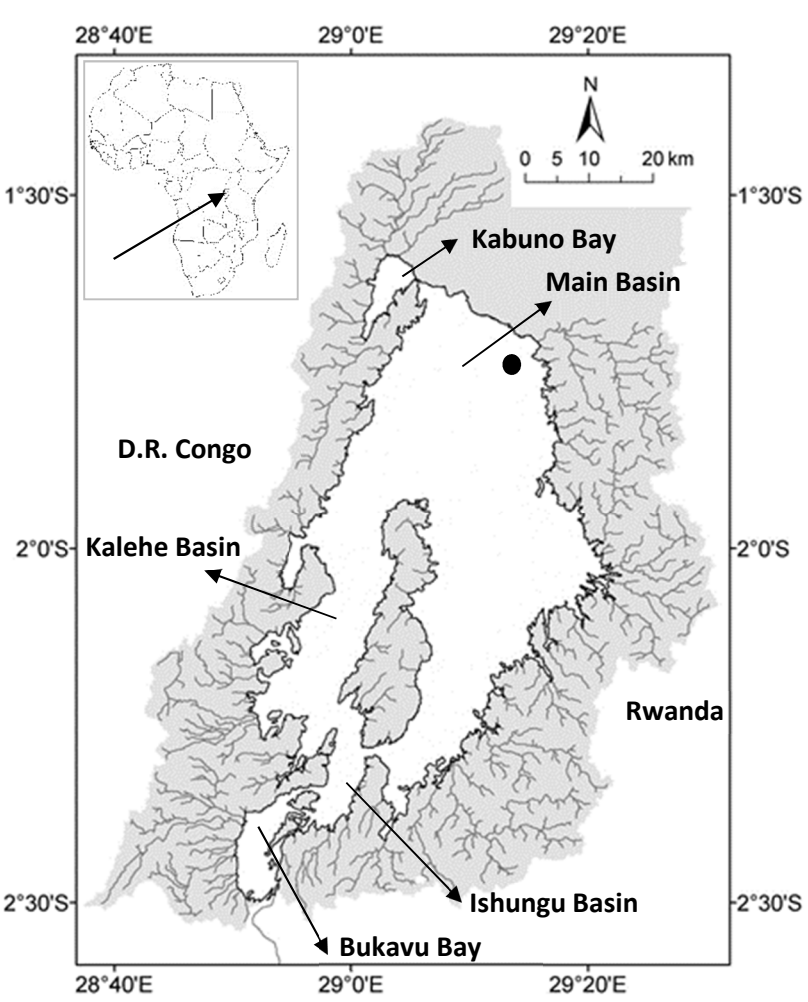

Figure 1: Map of Lake Kivu, showing the different basins and bays, and the sampling site in the main basin (black plot).

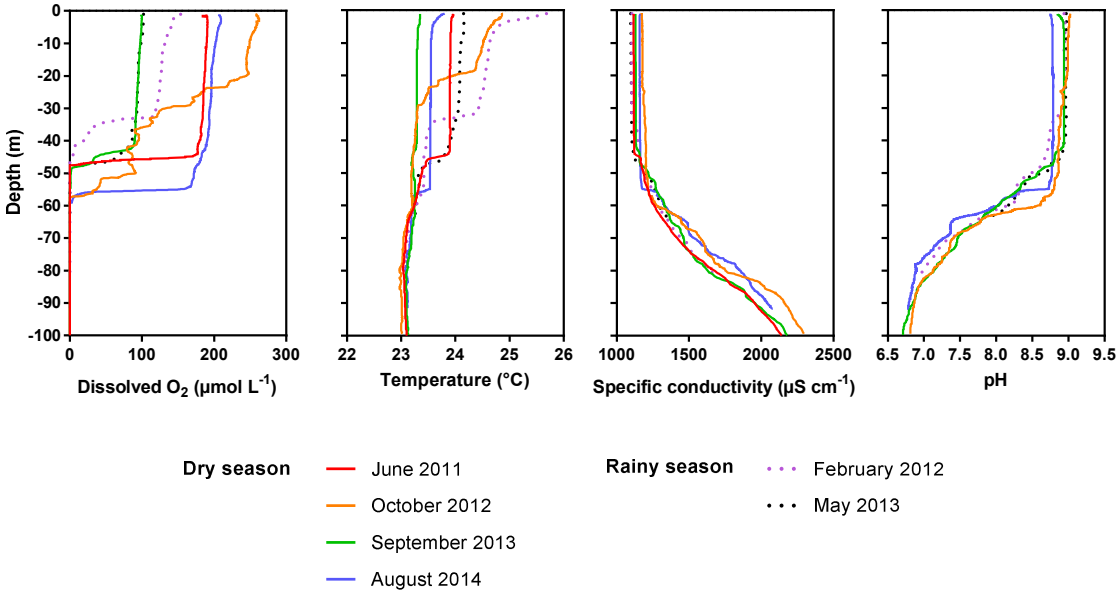

Figure 2: Vertical profiles of dissolved oxygen (µmol L^{-1}), temperature (°C), specific conductivity (µS cm^{-1}) and pH for the six field campaigns.

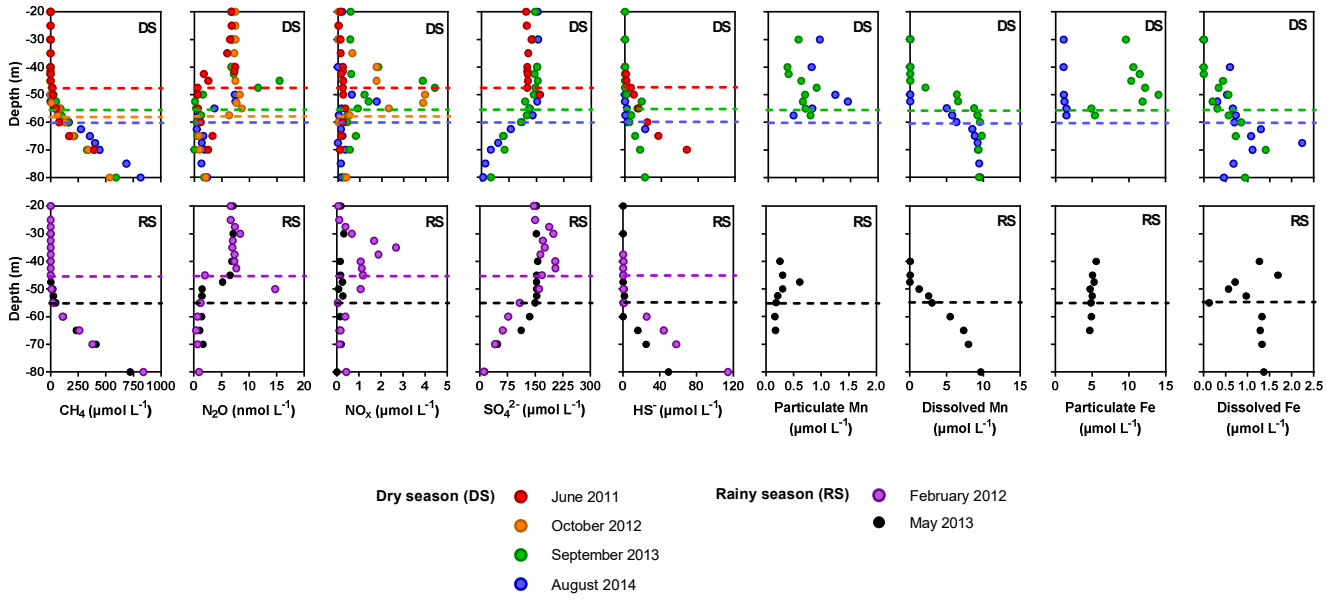

Figure 3: Vertical profiles of CH_4 (µmol L^{-1}), N_2O (nmol L^{-1}), NO_x (µmol L^{-1}), SO_4^{2-} (µmol L^{-1}), HS^- (µmol L^{-1}), particulate Mn and Fe (µmol L^{-1}) and dissolved Mn and Fe (µmol L^{-1}) concentrations for the six field campaigns. Horizontal dashed lines represent the anoxic layer for each season (same color code).

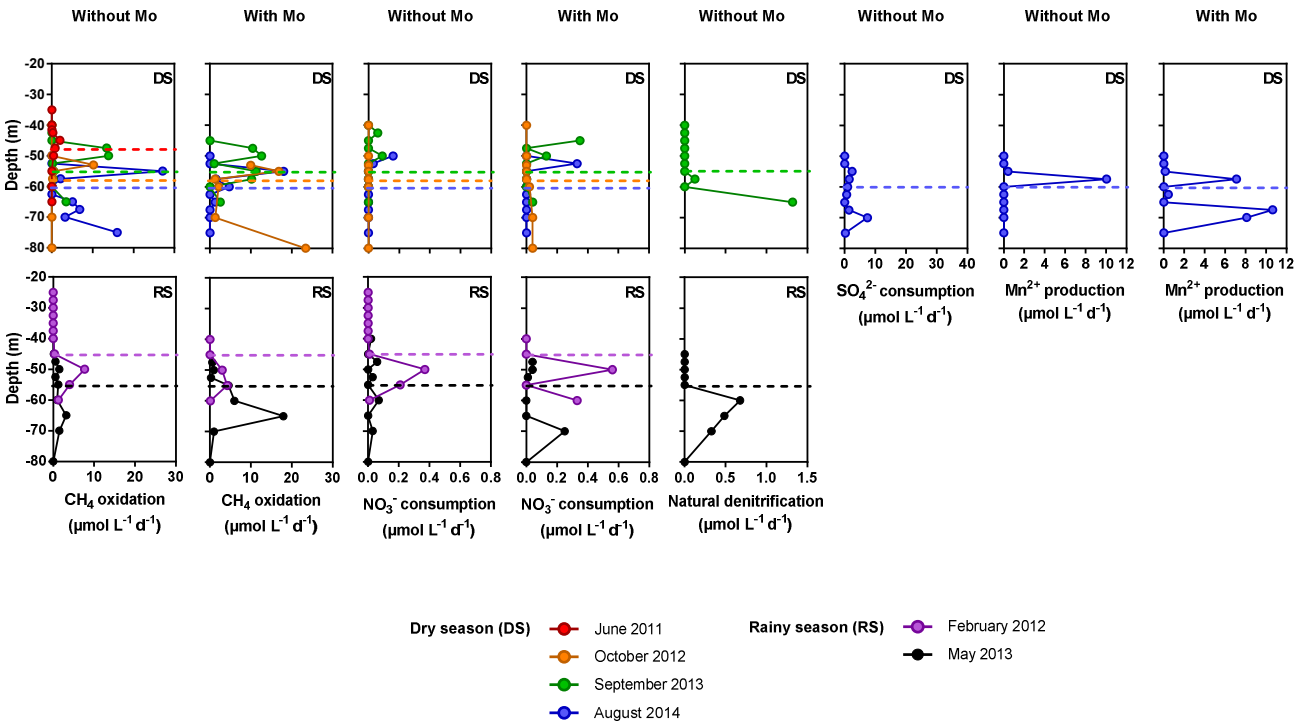

Figure 4: Process rates (CH_4 oxidation, NO_3^- consumption, Natural denitrification, SO_4^{2-} consumption and dissolved Mn production; µmol L^{-1} d^{-1}) without and with molybdate (Mo) added, during the six field campaigns (DS: dry season; RS: rainy season). Horizontal dashed lines represent the anoxic layer for each season (same color code).

625

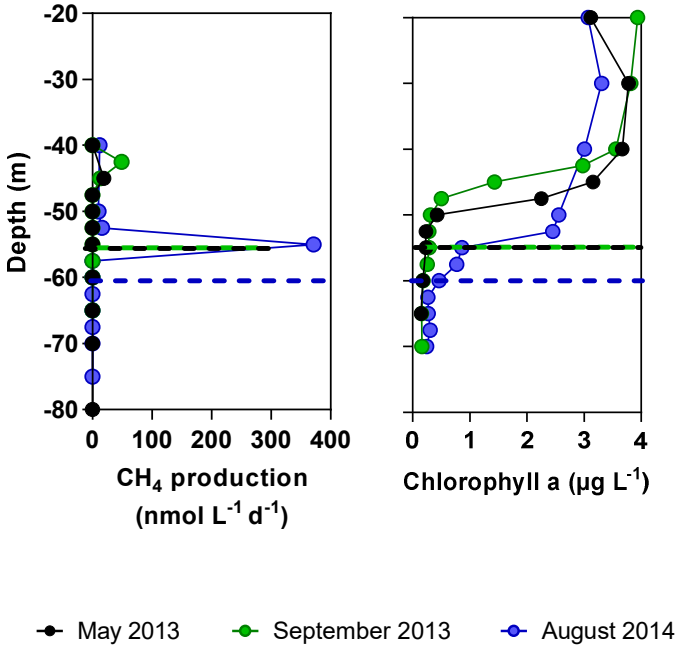

Figure 5: Vertical profiles of CH_4 production (nmol L^{-1} d^{-1}) and chlorophyll a concentration (µg L^{-1}) in May 2013 (black), September 2013 (green) and August 2014 (blue). The horizontal dashed lines represent the anoxic layer for each season (same color code).

630

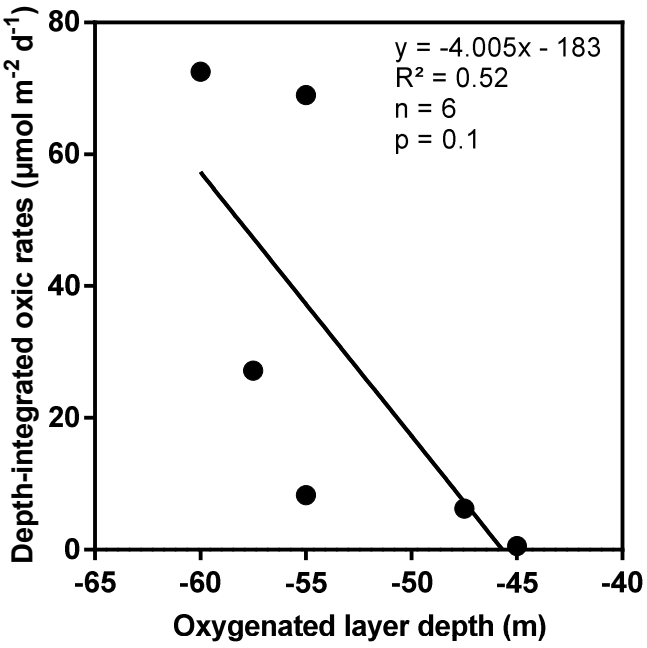

Figure 6: Depth-integrated aerobic CH_4 oxidation rates (µmol m^{-2} d^{-1}) compared to the oxygenated layer depth (m), for all field campaigns.

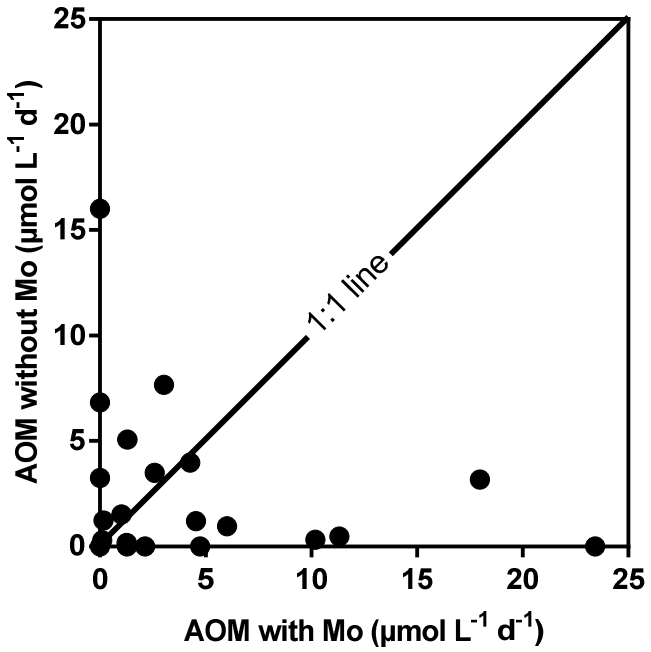

Figure 7: Comparison between AOM rates (µmol L^{-1} d^{-1}) measured without and with molybdate (Mo) added, during all field campaigns.

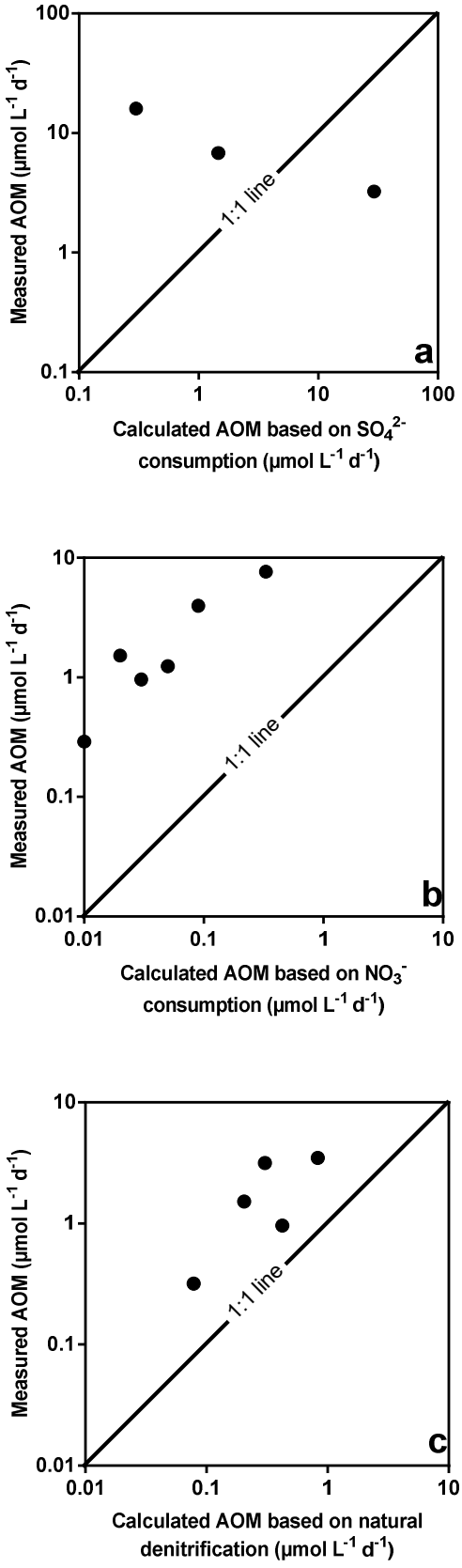

Figure 8: Comparison between measured and calculated AOM rates (µmol L^{-1} d^{-1}) based on (a) SO_4^{2-} consumption rates, (b) NO_3^- consumption rates and (c) Natural denitrification, for all field campaigns. Note the log scales.